CHAPTER 7

ETCHING AND KINETICS OF DISSOLUTION OF TaS_2 SINGLE CRYSTALS

CONTENTS PAGES

7.1	Introduction	127
7.2	Experimental	129
7.3	Observations	130
7.3.1	Etch pits and their orientation	130
7.3.2	Arrays of pits	131
7.3.3	Parallel slip lines	132
7.3.4	Network patterns	132
7.3.5	Pit density	133
7.4	Results	133
7.4.1	Effect of etching time	133
7.4.2	Effect of concentration	133
7.4.3	Dissolution kinetics	134
7.5	Discussion	136
7.6	References	139
	Captions of the figures	141
	Figures	142

7.1 Introduction

The physical, chemical and electrical properties of layered materials are influenced considerably by dislocations lying in the basal plane[1,2] but the importance of non-basal dislocations has only been recognised recently[3-5]. In graphite for example, non-basal dislocations of both screw and edge type, may be present in densities up to $10^5/cm^2$. The presence of such a high density of these defects in layered materials could well affect the establishment of certain parameters, like electrical resistivity[6-8], photoconductivity[9,10] and thermal conductivity.[11]

A great variety of liquid solutions have been used for etching and polishing of number of crystals, most of them being determined by a process of trial and error. Inspite of continuous efforts over years together in this field, the exact mechanism responsible for this process is not clearly understood. It is often true that many solutions, entirely different in composition of their constituents may give similar etching results, while with minor changes in the concentration or temperature, an etchant which revealed dislocation etch pits, may behave as a polishing solution and vice versa. It can also be said that the kinetics of etching may be reaction rate controlled in one solution and diffusion controlled in another.

In view of the increasing importance of single crystal of TaS_2 and the variety of behaviour observed in its various polytypic modifications, there is a pressing need for simple techniques that will reveal non-basal dislocations in these crystals. It is seen from the literature that there is no report regarding the etching of TaS_2 single crystals.

After several trials of various organic and inorganic acids, salts and their mixtures, an etchant capable of revealing the sites of emergence

of dislocations on (0001) face was developed. The tests for realiability of etchant, effect of concentration of etchant, pit morphology, effect of temperature on etch rates, reaction mechanism and other aspects of this phenomenon are studied, described and discussed in this chapter.

7.2 Experimental

Crystals were selected in the form of thin flat flakes with the c-axis perpendicular to the plane of the plates. After several trials, it was found that CrO_3 dissolved in double distilled water was capable to produce reliable etch pits. Etching solutions of different concentrations were prepared by dissolving analytical grade chromium trioxide in appropriate volume of double distilled water. The crystals were then immersed in an etchant kept in a 50 ml beaker at room temperature. The specimens were agitated for a measured time and then were immediately transferred to distilled water for cleaning. After being dried the specimens were observed under an optical microscope.

In order to study the effect of temperature, the specimens were subjected to etching by keeping them in a 50 ml etching solution contained

in a 100 ml beaker at constant temperatures (25° C - 65° C), in a constant temperature bath. The constant temperature was achieved by a toluene temperature regulator operated by a magnetic relay system. The temperature could be controlled to an accuracy of ± 0.5° C. Observations were recorded for various etching parameters like time, temperature and concentration. The specimen crystal was subjected to sequential etching and at the end of each etching stage, it was quenched and pit size was measured before re-immersion in an etchant for the next stage.

7.3 Observations

7.3.1 Etch pits and their orientation

As shown in Fig. 7.1 well defined characteristic dislocation etch pit patterns with clear background on the c-plane are observed on 1T-TaS_2 crystals, when they are etched in 10 N chromic acid solution at 65° C for 1 minute. The sides of these pits are always found to be parallel to the binary axes. The majority of the pits are symmetric, showing that dislocations are parallel to the c-axis. Flat bottomed pits are also observed quite often. The pit size is found to differ with different etching

parameters used. However, pits of different sizes are many times observed on the same surface. On prolonged etching these pits become larger in size and more or less preserve pyramidal shapes, though some of them become flat-bottomed and round-edged. The fact that etchant produces well defined pyramidal pits which retain their shapes while growing large on further etching strongly suggests that these pits are at the sites of emergence of dislocations on the surface.

7.3.2 Arrays of pits

In addition to the randomly distributed pits found on the etched surface, rows and columns of more or less equally spaced pits are also observed as shown in Fig. 7.2. The arrays of etch pits represent a linear arrangement of dislocations and in the absence of any surface step, the dislocations may have their Burgers vectors in the basal plane itself. The etch pits forming the linear arrays are equally spaced and approximately of the same shape and size. Such arrays of pits are typical of dislocation pits. The origin of such complex arrangement of dislocations intersecting (0001) face of 1T-TaS_2 crystal is not yet known to the author.

7.3.3 Parallel slip lines

Etching of the crystals has disclosed sets of parallel lines in which separation increases from one direction to the other and vice versa. This has been well illustrated in Figs. 7.3(a), 7.3(b) and 7.3(c).

The variation of the distance with some uniform rate may be attributed due to the variation of supersaturation or growth velocity during the growth of the crystals.

The parallel sets of lines are formed all over the surface suggesting their formation at the start of the growth of the crystals.

7.3.4 Net-work patterns

The c-plane being the easy slip plane in TaS_2, dislocation networks extending over the long distances would be formed in this plane. Figure 7.4 is the typical example of the interaction of the dislocation net-patterns observed on etched TaS_2 surfaces, showing crossing points of dislocations in the parallel glide planes as a result of interaction between them.

7.3.5 Pit density

The density of the pits varies from sample to sample and from one area of the sample to another. The extreme case of very high density of these pits is shown in Fig. 7.5(a). Figure 7.5(b) shows the etch pits developed on the opposite side of the crystal surface. Comparing these two etch patterns one can say that to a great extent baring few pits, there is a one-to-one correspondence in the positioning of pits.

Densities of non-basal dislocations were measured by counting the etch pits on different crystal samples. The variation of dislocation density was observed to be from 10^5 to 10^6 pits/cm^2.

7.4 Results

7.4.1 Effect of etching time

On successive etching the size of the pits was found to increase with the etching period. This is clear from plots of the etch-pit size versus time (Fig. 7.6).

7.4.2 Effect of concentration

The dependence of etch rate versus concentration is shown in Fig. 7.7. It is seen that the etch rate goes on decreasing with the increase in

the concentration of the etchant.

7.4.3 Dissolution kinetics

As is well known, the rate of all thermoactivated processes can be described by the Arrhenius equation

$$V = A e^{-E/kT}$$

where A is the pre-exponential factor, E the activation energy of the process, K the Boltzman's constant and T absolute temperature. The pre-exponential factor and the activation energy depend on the conditions of the experiment. The dependence of the log etch rate versus $\frac{1}{T}$ for dissolution of TaS_2 crystals in chromic acid solution of various concentrations is shown in Fig. 7.8.

The values of the dissolution activation energy and the pre-exponential factors as calculated from these graphs are given in Table 7.1. Both these values are found to decrease with the increase in the concentration of the etchant.

Plots of lnAd versus lnC and lnEα versus lnC have been made and are shown in

Table 7.1

Concentration	Activation energy (eV)	Pre-exponential factor (μm min^{-1})
20 N	0.1733	2.165×10^{-5}
14 N	0.2119	17.16×10^{5}
12 N	0.2284	54.48×10^{5}
10 N	0.2648	233.8×10^{5}

Figs. 7.9 and 7.10. From the straight line nature of the graphs it can be easily concluded that the pre-exponential factor A_d and the activation energy E_d have a C^k type dependence on the concentration C. The values of k obtained from the slopes of these graphs come to be −0.58 and −0.5 respectively.

7.5 Discussion

The process of dissolution may be diffusion controlled or reaction rate controlled. It depends upon the conditions of the experiment[12,13]. As a rule, the process controlled by reaction rate requires an activation energy in the 1 to 3 eV range[14]. The activation energy of dissolution is limited by diffusion changes in the 0.1 to 0.5 eV interval[12,15]. In the present case though the activation energy varies with concentration, it lies between 0.1 to 0.3 eV and therefore the process of dissolution is diffusion controlled.

From chemical kinetics theory it is known that the pre-exponential factor characterises the total number of collisions between reacting molecules. The fact that the pre-exponential factor decreases with the increase in the etchant concentration

suggests that the total number of collisions go on decreasing with the increasing concentration. One can therefore assume that the reaction products screen the crystal surface and hinder the adsorption of acid molecules on the surfaces. This point of view explains the decrease of pre-exponential factor with the increase in the concentration as observed in Fig. 7.9.

With the data available from Figs.7.7, 7.9 and 7.10 of the present work the equation of dissolution kinetics of TaS_2 can be written as

$$V_t = 7.64 \times 10^{12} \, C^{-5.8} \, e^{-0.789 \, C^{-0.5}/KT} \quad ..(7.1)$$

Values of V_t obtained from this equation after substituting the values of C, K and T are given in Table 7.2. When these values are compared with the experimentally observed values of V_t, it is seen that there is a reasonably good agreement between the two. This agreement justifies the validity of dissolution equation (7.1) written above.

Table 7.2

Dissolution etch rate (μm min⁻¹)	
V_t (cal.)	V_t (obs.)
227.0	238.5
470.0	459.0
596.0	612.5
736.6	795.0
315.4	325.0
697.0	662.0
911.4	893.0
1172.0	1290.0
386.1	399.5
887.7	848.0
1183.5	1160.0
1561.0	1740.0
467.0	475.0
1114.2	1080.0
1512.8	1514.0
2043.3	2350.0

7.6 References

1. Basinski, Z. S., Dove, D. B. and Mooser, E.
   Helv. Phys. Acta. 34 (1961) 373.

2. Basinski, Z. S., Dove, D. B. and Mooser, E.
   J. Appl. Phys. 34 (1963) 469.

3. Roscoe, C. and Thomas, J. M.
   Proc. Roy. Soc. A 297 (1967) 397.

4. Thomas, J. M. and Evans, E. L.
   Nature 214 (1967) 167.

5. Bahl, O. P., Evans, E. L. and Thomas, J.M.
   Proc. Roy. Soc. A 306 (1968) 53.

6. Fischer, G. and Brebner, J. L.
   J. Phys. Chem. Solids 23 (1962) 1363.

7. Tredgold, R. H. and Clark, A.
   Solid State Comm. 7 (1969) 1519.

8. Ismailov, F. I., Akhundov, G. A. and Vernich, O. R.
   Phys. Status Solidi 17 (1966) K 237.

9. Bube, R. H. and Lind, E. L.
   Phys. Rev. 115 (1959) 1159.

10. Brebner, J. L. and Fischer, G.
    Report Int. Conf. Physics of semiconductors (The Institute of Physical Society, London) (1962) 760.

11. Guseinov, G. D. and Rasulev, A. I.
    Phys. Status Solidi 18 (1966) 911.

12. Brodski, A. I.
Fiz. Khim. 2 (1948) 938.

13. Laider, K. J.
"Chemical Kinetics"
(McGraw Hill, New York) 1950.

14. "Kratkaya Khimicheskaya Entsiklopediya"
5 (Sovetskaya Entsiklopediya, Moscow, 1967).

15. Sangwal, K. and Arora, S. K.
J. Mater. Sci. 13 (1978) 1977.

Captions of the figures

Fig. 7.1	Well defined etch pits on TaS_2 crystals
Fig. 7.2	Etch pits observed in rows.
Figs.7.3(a), (b) and (c)	Sets of parallel lines observed during etching process.
Fig. 7.4	Net-work pattern observed on etched TaS_2 crystal surface.
Figs.7.5(a) and (b)	Etch pits developed on the opposite sides of a crystal.
Fig. 7.6	Plots of pit size versus etching time for ● - 20 N, O-14 N Δ - 12 N and ⊖ - 10 N at room temperature (25° C).
Fig. 7.7	Plots of etch rate versus concentration ● - 25°C O- 40°C, Δ - 50°C and ⊖ - 60 °C.
Fig. 7.8	Plots of log V versus 1/T for ● - 20 N O- 14 N, Δ -12 N and ⊖ - 10 N.
Figure 7.9	Plots of $\ln A_d$ versus $\ln C$.
Fig. 7. 10	Plots of $\ln E_d$ versus $\ln C$.

Fig. 7.1 X 264

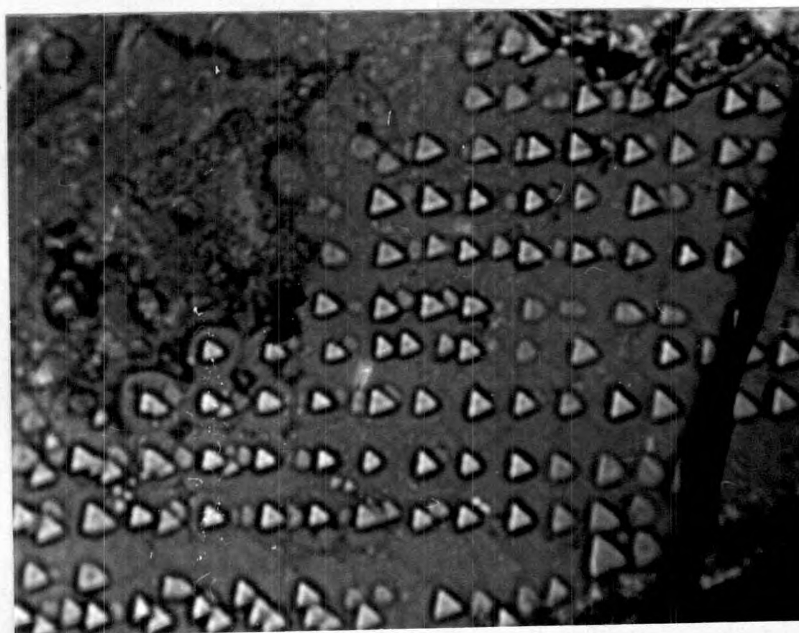

Fig. 7.2 X 216

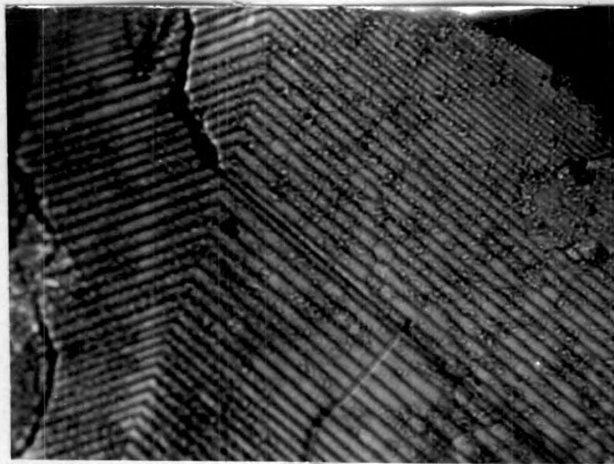

Fig. 7.3(a) X 192

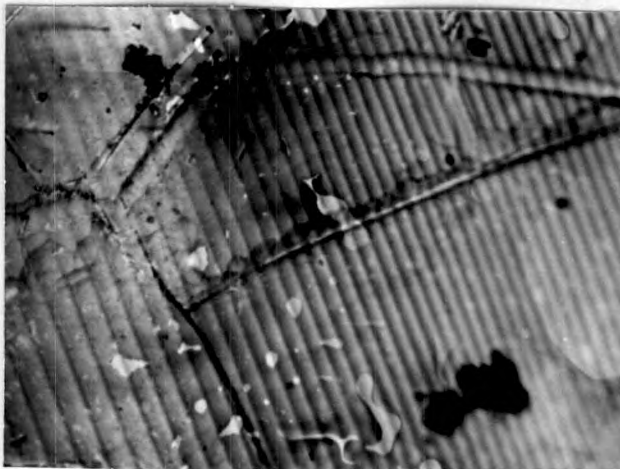

Fig. 7.3(b) X 240

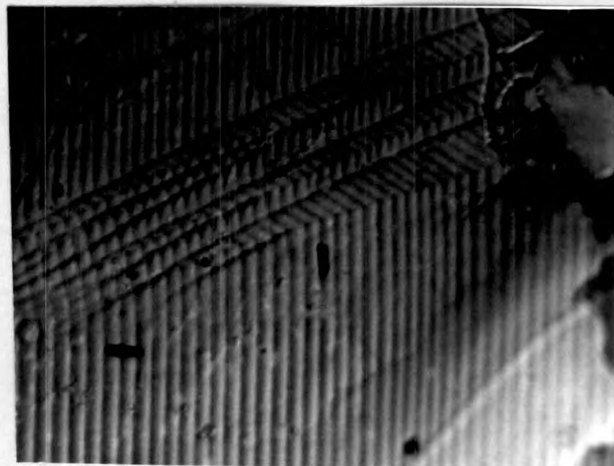

Fig. 7.3(c) X 144

Fig. 7.4 X 192

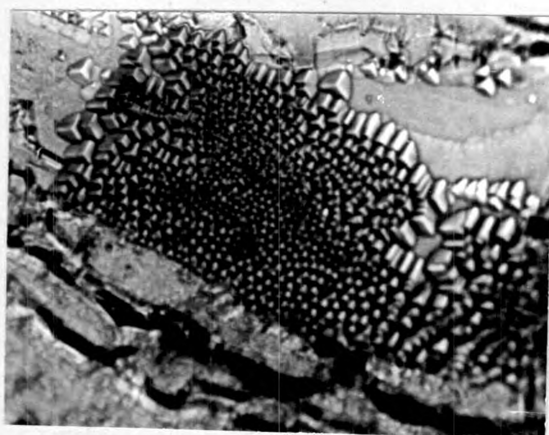

Fig. 7.5(a) X 120

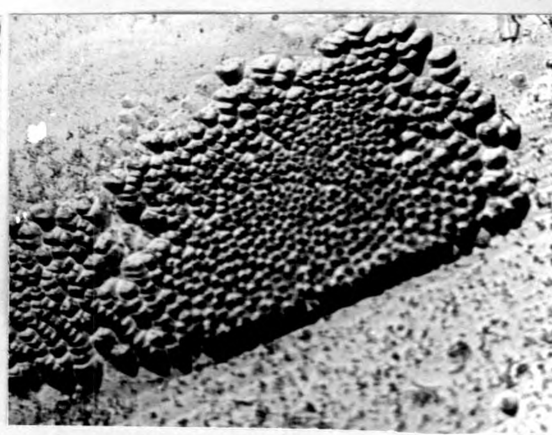

Fig. 7.5(b) X 120

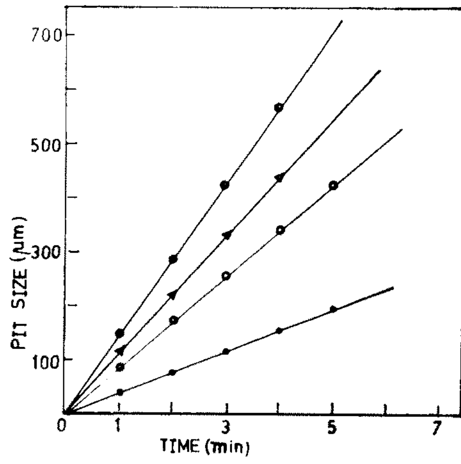

Fig. 7.6

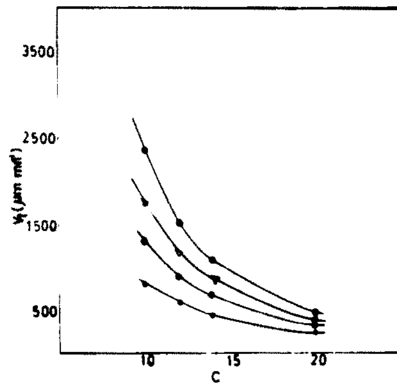

Fig. 7.7

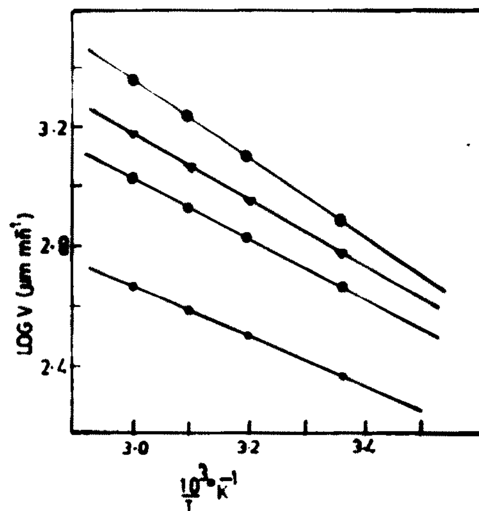

Fig. 7.8

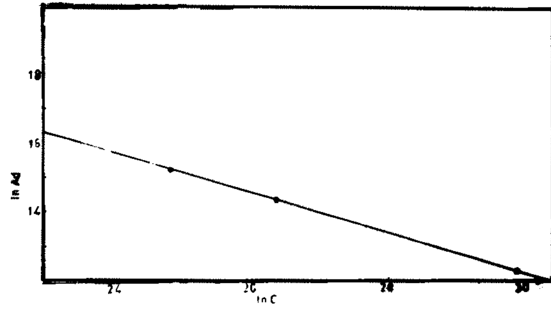

Fig. 7.9

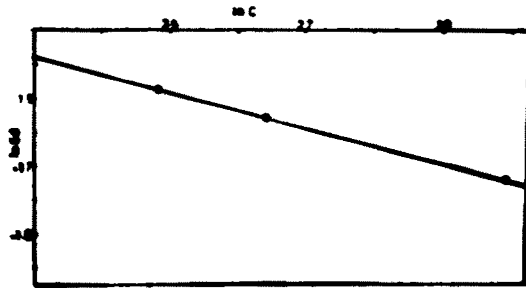

Fig. 7.10